Pergamon

Int. J. Solids Structures Vol. 34, No. 28, pp. 3643–3656, 1997

0020–7683/97 $17.00 + .00

PII: S0020–7683(96)00235–1

THERMAL STRESS EVOLUTION IN CONTINUOUSLY QUENCHED CIRCULAR BARS

YIMIN RUAN
Alcoa Technical Center, Aluminum Company of America, 100 Technical Drive, Alcoa Center, PA 15069, U.S.A.

(*Received* 26 *May* 1996; *in revised form* 18 *November* 1996)

Abstract—This paper presents a finite element method for studying continuous quenching processes with emphasis on thermal and stress analyses of axisymmetric problems. Both the thermal and stress problems involved in the quenching process are formulated in the Eulerian frame. The heat transfer problem is solved with the Petrov-Galerkin method due to the convetion-diffusion nature of the governing equation. For the thermal stress problem, since the acceleration term in the equation of motion is small, it is neglected and the equilibrium equation is solved. The inelastic deformation associated with the quenching process is modeled with the visco-plastic type of constitutive laws. To determine the inelastic deformation of the quenched body, the inelastic strain rates are integrated along the quenched body with the Petrov-Galerkin formulation applied to the material derivatives of the inelastic strain rates. An example problem for a continuous bar quenching process is studied with the method presented in this paper. With the present method, computational time needed is significantly less than that with Lagrangian approaches. © 1997 Elsevier Science Ltd.

INTRODUCTION

Continuous quenching processes are widely used in industry. The advantage of the continuous quenching process is its high productivity. During the quenching process, a certain level of cooling rate must be maintained in order to obtain proper material properties. Due to non-uniform temperature in a quenched body, high thermal stresses are induced. The thermal stresses remaining in the body after the quenching process (or residual stresses) are undesirable since they may cause excess distortion of a finished product. The unpredictable distortion of a part after a machining process caused by the residual stresses may result in rejection of the part. Furthermore, the residual stresses may have a deleterious effect on fracture and corrosion performance. Therefore, understanding the stress evolution is important to obtain quality products.

Traditionally, quenching processes are studied through transient analyses, although many industrial quenching processes are continuous, or semi-continuous. Examples for non-continuous transient analyses can be found in the references by Fletcher and Lewis (1985), Zabaras *et al.* (1987) and Becker *et al.* (1994). The transient approaches may not be very desirable to simulate the continuous quenching process because of the variation of the cooling conditions at a material point on a cooling boundary. In addition, with the transient approaches, the computational domain must be much larger than that interested, so that extra computation is required. To overcome the drawbacks of the transient approaches, a method is developed in this paper to simulate the continuous quenching process with emphasis on steady state (or quasi-steady state) analysis.

THERMAL ANALYSIS

Governing equation and boundary conditions

The equation that governs the heat transfer for a circular bar under the axisymmetric conditions is as follows:

$$\rho c\left(V_r\frac{\partial T(r,z)}{\partial r}+V_z\frac{\partial T(r,z)}{\partial z}\right)=\frac{1}{r}\frac{\partial}{\partial r}\left(kr\frac{\partial T(r,z)}{\partial r}\right)+\frac{\partial}{\partial z}\left(k\frac{\partial T(r,z)}{\partial z}\right)\quad (r,z)\in\Omega \tag{1}$$

where ρ, c and k are the density, specific heat and conductivity, respectively; r and z are the radial and axial coordinates (Fig. 1); V_r and V_z are the steady state radial and axial velocity components, respectively; and Ω is the control volume.

Before the bar is quenched, it is heated up to a uniform temperature, T_u. During the process, the bar moves at a constant velocity, $V=(V_r, V_z)$, through a quenching chamber where the bar emerges into a quenching medium. Therefore, at the upstream of the control volume, the temperature condition must be satisfied, i.e., $T(r,z)=T_u$, where $(r,z)\in\partial\Omega_u$, and the convection and radiation boundary conditions can be used to represent the cooling effect at the surface of the bar, i.e., $-k\partial T(r,z)/\partial n=h(T-T_\infty)+R(T^4-T_\infty^4)$, where $(r,z)\in\partial\Omega_c$, h and R are the convection and radiation heat transfer coefficient, respectively; and T_∞ is the environmental temperature (the temperature of the cooling medium). Here $\partial\Omega_c$ represents the surface of the bar where it is cooled and $\partial\Omega_u$ denotes the upstream boundary of the control volume.

Finite element formulation of the heat transfer problem

Since standard Galerkin method may lead to unstable solutions for convection-diffusion problems with high Peclet numbers, the Petrov-Galerkin approach is used for the heat transfer analysis. With the trial and test functions T, $\bar{T}\in V=\{v\in H_0^1\}$, where H_0^1 is a Soblev space, the following variational statement can be derived from the governing equation for the heat transfer problem, eqn (1):

$$\int_\Omega \rho c\left(V_r\frac{\partial T}{\partial r}+V_z\frac{\partial T}{\partial z}\right)\left(\bar{T}+\left(\delta_r\frac{\partial\bar{T}}{\partial r}+\delta_z\frac{\partial\bar{T}}{\partial z}\right)\right)d\Omega+\int_\Omega k\left(\frac{\partial T}{\partial r}\frac{\partial\bar{T}}{\partial r}+\frac{\partial T}{\partial z}\frac{\partial\bar{T}}{\partial z}\right)d\Omega$$
$$-\int_\Omega\left(\frac{1}{r}\frac{\partial}{\partial r}\left(kr\frac{\partial T(r,z)}{\partial r}\right)+\frac{\partial}{\partial z}\left(k\frac{\partial T(r,z)}{\partial z}\right)\right)\left(\delta_r\frac{\partial\bar{T}}{\partial r}+\delta_z\frac{\partial\bar{T}}{\partial z}\right)d\Omega-\int_{\partial\Omega}k\frac{\partial T}{\partial n}\bar{T}\,d\Gamma=0 \tag{2}$$

where δ_r and δ_z are the function of the element size and velocity, $d\Omega=r\,dr\,dz$ and $d\Gamma=r\,ds(ds=\sqrt{dr^2+dz^2})$.

To obtain the finite element discretization, the control volume Ω is divided into E elements and M nodes, and the temperature in the domain is represented with interpolation functions. The interpolation function for the temperature can be expressed as $T=\Sigma T_a\Phi_a$, $(a=1,2,\ldots,M)$, where T_a are the nodal temperatures, and Φ_a are the isoparametric finite element shape functions. The function $\bar{T}$ can also be expressed with the finite element shape function as $\bar{T}=\Sigma\bar{T}_a\Phi_a$, where $\bar{T}_a$ are the nodal values of $\bar{T}$. Based on the element size and steady state velocity, the functions δ_r and δ_z can be defined as $\delta_r=0.5(\coth Pe-1/Pe)sV_r/|V|$

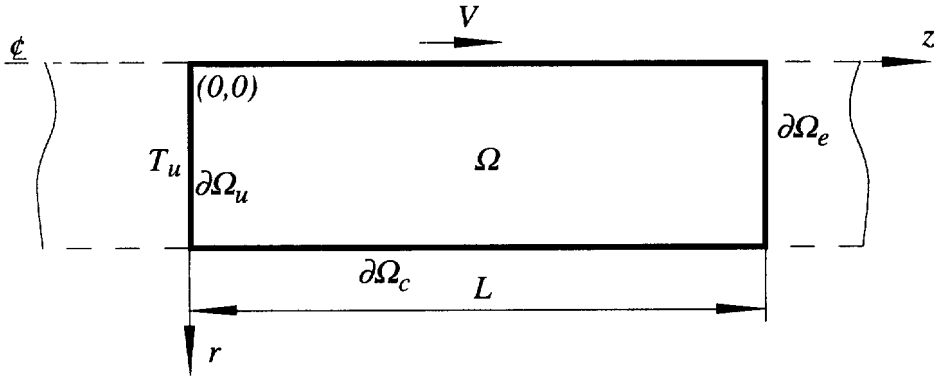

Fig. 1. Schematic diagram of the quenched circular bar.

and $\delta_z = 0.5(\coth Pe - 1/Pe)sV_z/|V|$, where s is the element size and $Pe = 0.5|V|s/k$ (Zienkiewicz and Taylor (1991), Kikuchi (1986)). After the finite element discretization, the following system of equations can be obtained:

$$\mathbf{KT} = \mathbf{F} \tag{3}$$

where $\mathbf{K}$ and $\mathbf{F}$ are the stiffness matrix and load vector, respectively; and $\mathbf{T}$ is the vector of temperatures at nodal points. The components of $\mathbf{K}$ and $\mathbf{F}$ are

$$K_{ab} = \int_\Omega \rho c\left(V_r\frac{\partial\Phi_b}{\partial r} + V_z\frac{\partial\Phi_b}{\partial z}\right)\left(\Phi_a + \left(\delta_r\frac{\partial\Phi_a}{\partial r} + \delta_z\frac{\partial\Phi_a}{\partial z}\right)\right)\mathrm{d}\Omega$$
$$+ \int_\Omega k\left(\frac{\partial\Phi_a}{\partial r}\frac{\partial\Phi_b}{\partial r} + \frac{\partial\Phi_a}{\partial z}\frac{\partial\Phi_b}{\partial z}\right)\mathrm{d}\Omega + \int_{\partial\Omega_c}(h + a_r(T, T_\infty))\Phi_a\Phi_b\,\mathrm{d}\Gamma$$
$$- \int_\Omega\left(\frac{1}{r}\frac{\partial}{\partial r}\left(kr\frac{\partial\Phi_b}{\partial r}\right) + \frac{\partial}{\partial z}\left(k\frac{\partial\Phi_b}{\partial z}\right)\right)\left(\delta_r\frac{\partial\Phi_a}{\partial r} + \delta_z\frac{\partial\Phi_a}{\partial z}\right)\mathrm{d}\Omega \tag{4}$$

$$F_a = \int_{\partial\Omega_c}(T_\infty + a_r(T, T_\infty)T_\infty)\Phi_a\,\mathrm{d}\Gamma \tag{5}$$

where $a_r(T, T_\infty)$ is the equivalent heat transfer coefficient for radiation and is defined as $a_r(T, T_\infty) = R(T^2 + T_\infty^2)(T - T_\infty)$. Notice that when k is constant, some of the high order terms in eqn (4) will vanish when the linear or bi-linear elements are used. More discussions on the calculation of the high order term can be found in the book by Johnson (1987).

STRESS ANALYSIS

Governing equations

Generally, the acceleration term in the equation of motion is small for the quenching problems and can be neglected. This will lead to the same equilibrium equation as that used for static analyses, that is,

$$-\frac{1}{r}\frac{\partial}{\partial r}(r\sigma_r) - \frac{\partial}{\partial z}(\sigma_{rz}) + \frac{1}{r}\sigma_\theta = 0 \tag{6}$$

$$-\frac{1}{r}\frac{\partial}{\partial r}(r\sigma_{rz}) - \frac{\partial}{\partial z}(\sigma_z) = 0 \tag{7}$$

where σ_r, σ_z, σ_{rz} and σ_θ are the components of the vector form of the Cauchy stress tensor. The body force is neglected in the above equations.

For the quenching problem studied here with small strains and rotations, we can reasonably assume that the total strain tensor $\boldsymbol{\varepsilon}$ can be additively decomposed into the elastic, $\boldsymbol{\varepsilon}^E$, the thermal, $\boldsymbol{\varepsilon}^T$, and the inelastic, $\boldsymbol{\varepsilon}^N$, part, respectively, that is,

$$\boldsymbol{\varepsilon} = \boldsymbol{\varepsilon}^E + \boldsymbol{\varepsilon}^T + \boldsymbol{\varepsilon}^N \tag{8}$$

where $\boldsymbol{\varepsilon}$ is the total strain tensor with the vector form $\boldsymbol{\varepsilon} = (\varepsilon_r\,\varepsilon_z\,\varepsilon_{rz}\,\varepsilon_\theta)^T$, $\boldsymbol{\varepsilon}^E$, $\boldsymbol{\varepsilon}^T$ and $\boldsymbol{\varepsilon}^N$ are the elastic, the thermal, and the inelastic strain, respectively, and they have the same form as $\boldsymbol{\varepsilon}$ does. The total strain tensor can be calculated through the displacement field as $\varepsilon_r = \partial u_r/\partial r$, $\varepsilon_z = \partial u_z/\partial z$, $\varepsilon_\theta = u_r/r$, $\varepsilon_{rz} = 0.5\gamma_{rz} = 0.5(\partial u_r/\partial z + \partial u_z/\partial r)$.

To model the stress evolution, the following constitutive equation for elastic deformation is used:

$$\boldsymbol{\sigma} = \mathbf{D}(T)\boldsymbol{\varepsilon}^E \tag{9}$$

where $\boldsymbol{\sigma}$ is the vector form of the Cauchy stress tensor, i.e., $\boldsymbol{\sigma} = (\sigma_r \sigma_z \sigma_{rz} \sigma_\theta)^T$, and $\mathbf{D}(T)$ is the temperature dependent elastic constant tensor and its matrix form is given as

$$\mathbf{D} = \frac{E(T)}{(1+\nu)(1-2\nu)} \begin{bmatrix} 1-\nu & \nu & 0 & \nu \\ \nu & 1-\nu & 0 & \nu \\ 0 & 0 & \dfrac{(1-2\nu)}{2} & 0 \\ \nu & \nu & 0 & 1-\nu \end{bmatrix} \tag{10}$$

where $E(T)$ is the Young's modulus and ν is the Poisson's ratio.

Thermal strains are dilatational and can be expressed as

$$\varepsilon_r^T(T) = \varepsilon_z^T(T) = \varepsilon_\theta^T(T) = \int_{T_R}^{T} a(\nu)\,\mathrm{d}\nu, \quad \varepsilon_{rz}^T(T) = 0 \tag{11}$$

where $a(T)$ is the temperature dependent coefficient of thermal expansion and T_R is the reference temperature at which the thermal strains are zero.

To model the inelastic deformation, the visco-plastic type of constitutive laws is used in the example problem presented later. The visco-plastic law has the following form:

$$\dot{\boldsymbol{\varepsilon}}^N = \mathbf{f}(\boldsymbol{\sigma}, T). \tag{12}$$

The methodology developed here is not limited to this type of constitutive law, generally, any laws that model the variation of strains with respect to time can be used.

Virtual work and finite element formulation

Applying the virtual work principle to eqns (6) and (7), one can derive the following weak formulation:

$$\int_\Omega \boldsymbol{\sigma}(\mathbf{u}) : \boldsymbol{\varepsilon}(\bar{\mathbf{u}})\,\mathrm{d}\Omega = \int_{\partial\Omega} \boldsymbol{\tau} \cdot \bar{\mathbf{u}}\,\mathrm{d}\Gamma \tag{13}$$

where $\mathbf{u}(\mathbf{u} = (u_r u_z)^T)$ is the displacement field and $\bar{\mathbf{u}}$ is virtual displacement field.

Although the finite element analysis of the stress problem can be performed with the same discretization as that used for the heat transfer analysis, we consider a general case with a different finite element discretization. Assuming that the control volume is discretized with N nodes and E elements, one can express the displacement field with isoparametric shape functions $\mathbf{N}$ as $\mathbf{d} = \mathbf{N}\mathbf{u}$. The corresponding strain and stress fields are $\boldsymbol{\varepsilon} = \mathbf{B}\mathbf{u}$ and $\boldsymbol{\sigma} = \mathbf{D}\mathbf{B}\mathbf{u}$, respectively, where $\mathbf{B}$ is derived through differentiation of the shape function $\mathbf{N}$. After the discretization and using eqns (8) and (9), one can derive the following system of equations from eqn (13):

$$\int_\Omega \mathbf{B}^T\mathbf{D}\mathbf{B}\,\mathrm{d}\Omega\mathbf{u} = \int_{\partial\Omega} \mathbf{B}^T\boldsymbol{\tau}\,\mathrm{d}\Gamma + \int_\Omega \mathbf{B}^T\mathbf{D}(\boldsymbol{\varepsilon}^T + \boldsymbol{\varepsilon}^N)\,\mathrm{d}\Omega \tag{14}$$

where $\mathrm{d}\Omega = r\,\mathrm{d}r\,\mathrm{d}z$. The compact from the above equation can be written as

$$\mathbf{AU} = \mathbf{P} \tag{15}$$

where **A** is the stiffness matrix, **U** is the vector of the displacement field, and **P** is the load vector.

CALCULATION OF INELASTIC STRAINS

In the development here, materials with visco-plastic behaviors are considered with the material inelastic deformation represented by eqn (12). Generally, any rate type of constitutive laws can be applied.

Using the material derivative of the inelastic strain rate, $\dot{\varepsilon}^N = \partial\varepsilon^N/\partial t + V_r\partial\varepsilon^N/\partial r + V_z\partial\varepsilon^N/\partial z$, and eqn (12), one can derive the following equation:

$$\frac{\partial\varepsilon^N}{\partial t} + V_r\frac{\partial\varepsilon^N}{\partial r} + V_z\frac{\partial\varepsilon^N}{\partial z} = f(\sigma, \varepsilon^N, T) \tag{16}$$

where t is the time.

In the quenching problem, the mechanical deformation is induced mainly by temperature gradient in the quenched body and the velocity due to mechanical deformation is negligible comparing with the rigid body velocity (steady state moving velocity of a quenched body). Therefore, the rigid body velocity can be used in the above equation.

Equation (16) represents the evolution of inelastic strain with time. For the steady state quenching process, to an observer in the Eulerian frame, $\partial\varepsilon^N/\partial t = 0$. In this analysis, the term $\partial\varepsilon^N/\partial t$ is kept for the purpose of iteration.

Before the quenched body enters the quenching chamber, it has a uniform temperature. At this stage, there is no deformation in the body. Therefore, the value of the total inelastic strains at the upstream of the control volume Ω is

$$\varepsilon^N = 0 \quad \text{on } \partial\Omega_u \tag{17}$$

The inelastic deformation is history dependent, which requires the integration of the inelastic strain rates. To integrate the inelastic strain rates, a weak formulation can be applied to eqn (16) on the control volume Ω. When the standard Galerkin method is used, the finite element method results in centered finite difference schemes when the mesh is uniform because of the usual basis functions (hat function). It can be shown that the system developed with the standard Galerkin method is unstable. Therefore, the Petrov-Galerkin method is used in this analysis. The variational statement of eqn (16) with Petrov-Galerkin method is as follows:

$$\int_\Omega \left(\frac{\partial\varepsilon^N}{\partial t} + V_r\frac{\partial\varepsilon^N}{\partial r} + V_z\frac{\partial\varepsilon^N}{\partial z}\right)\left\{w + \gamma\xi\left(V_r\frac{\partial w}{\partial r} + V_z\frac{\partial w}{\partial z}\right)\right\} \mathrm{d}A = \int_\Omega f(\sigma, T)\left\{w + \gamma\xi\left(V_r\frac{\partial w}{\partial r} + V_z\frac{\partial w}{\partial z}\right)\right\} \mathrm{d}A \tag{18}$$

where $w \in V = \{v \in H_0^1\}$ (H_0^1 is a Soblev space) and ξ is the element parameter. Notice that eqn (18) can be considered as the summation of two equations with the standard Galerkin method for two different test functions, i.e., w and $\gamma\xi(V_r\partial w/\partial r + V_z\partial w/\partial z)$. The proof of stability of the Petrov-Galerkin method can be found in references by Johnson (1987) and Pironneau (1989).

Equation (18) can be discretized with the finite element interpolation functions for the inelastic strains and the function w as $\varepsilon^N = \Sigma\varepsilon_\beta^N\Psi_\beta$, $w = \Sigma w_\beta\Psi_\beta$ ($\beta = 1, 2, \ldots, L$), respectively, where L is the number of nodes, ε_β^N are the nodal values of the inelastic strain tensor,

and Ψ_β are shape functions which may be the same as, or different from those used for temperature and displacement interpolations. Generally, integration of the inelastic strains can be performed with the mesh used for thermal analysis or for stress analysis. Using the finite element interpolation functions, from eqn (18), one can derive the following equation:

$$\int_\Omega \left\{\Psi_\alpha + \gamma\xi\left(V_r\frac{\partial\Psi_\alpha}{\partial r} + V_z\frac{\partial\Psi_\alpha}{\partial z}\right)\right\}\Psi_\beta \,\mathrm{d}A\frac{\partial\varepsilon_\beta^N}{\partial t} + \int_\Omega \left\{\Psi_\alpha + \gamma\xi\left(V_r\frac{\partial\Psi_\alpha}{\partial r} + V_z\frac{\partial\Psi_\alpha}{\partial z}\right)\right\}\left(V_r\frac{\partial\Psi_\beta}{\partial r} + V_z\frac{\partial\Psi_\beta}{\partial z}\right)\mathrm{d}A\varepsilon_\beta^N = \int_\Omega \left\{\Psi_\alpha + \gamma\xi\left(V_r\frac{\partial\Psi_\alpha}{\partial r} + V_z\frac{\partial\Psi_\alpha}{\partial z}\right)\right\} f(\boldsymbol{\sigma}, T)\,\mathrm{d}A. \quad (19)$$

The above equation can be written in the following compact form:

$$\mathbf{C}\dot{\mathbf{e}} + \mathbf{Q}\mathbf{e} = \mathbf{g} \quad (20)$$

where the vector $\mathbf{e}$ contains inelastic strains, the components of the vector $\mathbf{g}$ is

$$g_\alpha = \int_\Omega \left\{\Psi_\alpha + \gamma\xi\left(V_r\frac{\partial\Psi_\alpha}{\partial r} + V_z\frac{\partial\Psi_\alpha}{\partial z}\right)\right\} f(\boldsymbol{\sigma}, T)\,\mathrm{d}A \quad (21)$$

and the components of the matrices $\mathbf{C}$ and $\mathbf{Q}$ are

$$C_{\alpha\beta} = \int_\Omega \left\{\Psi_\alpha + \gamma\xi\left(V_r\frac{\partial\Psi_\alpha}{\partial r} + V_z\frac{\partial\Psi_\alpha}{\partial z}\right)\right\}\Psi_\beta \,\mathrm{d}A \quad (22)$$

$$Q_{\alpha\beta} = \int_\Omega \left\{\Psi_\alpha + \gamma\xi\left(V_r\frac{\partial\Psi_\alpha}{\partial r} + V_z\frac{\partial\Psi_\alpha}{\partial z}\right)\right\}\left(V_r\frac{\partial\Psi_\beta}{\partial r} + V_z\frac{\partial\Psi_\beta}{\partial z}\right)\mathrm{d}A. \quad (23)$$

Equation (20) can be integrated with the backward Euler scheme as

$$\left(\frac{\mathbf{C}}{\Delta t} + \mathbf{Q}\right)\mathbf{e}^n = \mathbf{g} + \frac{\mathbf{C}}{\Delta t}\mathbf{e}^{n-1} \quad (24)$$

where n represents the current step number.

The term $\mathbf{C}\mathbf{e}^{n-1}$ in the above equation is related to the inelastic strains at the previous step. When the term $\mathbf{C}\mathbf{e}^{n-1}$ is combined with the load vector $\mathbf{g}$ to form a modified load vector $\mathbf{g}^*$, the following equation can be obtained,

$$\left(\frac{\mathbf{C}}{\Delta t} + \mathbf{Q}\right)\mathbf{e}^n = \mathbf{g}^* \quad (25)$$

where the components of $\mathbf{g}^*$ are

$$g_\alpha^* = \int_\Omega \left\{\Psi_\alpha + \gamma\xi\left(V_r\frac{\partial\Psi_\alpha}{\partial r} + V_z\frac{\partial\Psi_\alpha}{\partial r}\right)\right\}\left(f(\sigma, T) + \frac{(\varepsilon^N)^{n-1}}{\Delta t}\right)\mathrm{d}\Omega. \tag{26}$$

Notice that **Q** and **C** are independent of the inelastic strains, if Δt is kept constant, the stiffness matrix will not vary during interations. Therefore, matrix forward elimination during iterations is not necessary.

RESULTS

In this section, an axisymmetric bar quenching problem is studied. The diameter of the bar is 0.03 m. The control volume is as shown in Fig. 1, where the length of the control volume is $L = 0.7$ m. The steady state velocity is $\mathbf{V} = (0, 0.15)$ m/sec. The water cooling starts at $x = 0.06$ m and ends at $x = 0.46$ m with a total cooling zone 0.4 m. The water cooling heat transfer coefficient is $h = 14{,}200$ W/m^2°C for 0.06 m $\leqslant x \leqslant$ 0.46 m, and the rest of the bar surface is cooled by the surrounding air with $h = 30$ W/m^2°C, the sink temperature is $T_\infty = 25$°C. Before the bar enters the quenching chamber, it is kept at a uniform temperature at $T_u = 510$°C. With the assumption of uniform cooling around the bar surface, symmetric conditions can be applied along the center line of the bar. The traction free condition is applied to the bar surface and at the end of the control volume at $x = 0.7$ m. At the upstream of the control volume, the point at (0, 0) is fixed in order to eliminate the rigid body mode.

The thermal properties of the bar (A1 1100) are: $k = 222$ W/m-°C, $c = 904$ J/kg-°C, $\rho = 2650$ kg. The mechanical properties are: $E(T) = 7310 - 48.6\,T$ MPa if $T \leqslant 340$°C and $E(T) = 103{,}000 - 139\,T$ MPa if $T > 340$°C, $v = 0.37$, $\alpha(T) = 25.5$ μm/m.

In the problem studied here, the hyperbolic-sine law is used, which has the following form:

$$\dot{\varepsilon}_{ij}^N = \frac{3}{2}Ae^{-c/T+273}[\sinh B\bar{\sigma}]^n\frac{s_{ij}}{\bar{\sigma}} \tag{27}$$

where A, B, C and n are the material constants, $\bar{\sigma}$ is the effective stress defined as $\bar{\sigma} = \sqrt{\frac{3}{2}s_{ij}s_{ij}}$ (s_{ij} are the deviatoric stresses and are defined as $s_{ij} = \sigma_{ij} - \frac{1}{3}\sigma_{kk}\delta_{ij}$). The temperature T is in degrees Celsius. The parameters of the Hyperbolic-sine law for A1 1100 are $A = 8.557 \times 10^{12}$ sec^{-1}, $B = 0.03223$ MPa^{-1}, $C = 21{,}320$°K, and $n = 4.75$ (Becker *et al.* (1994)).

To verify the methodology presented in this paper, the transient (Lagrangian) analysis is performed with the commercial program ABAQUS (1995), and the temperatures and stresses are plotted with both the transient and steady state methods.

Figure 2 shows the temperature variation along the bar at various locations in the radial direction. Figures 3 and 4 show the stress evolution along the bar at two different locations in the radial direction, i.e., $r = 0.005255$ m and $r = 0.01469$ m. The solid black symbols in Figs 2–4 indicate the transient solutions obtained with ABAQUS. A good agreement between the steady state and the transient solutions can be seen from these figures. The small discrepancy in stresses may be due to the stress output points where the stresses computed with ABAQUS are output at the nodal points and stresses calculated with the present method is output at the center of elements.

Figures 5 and 6 show the strain rates along the bar at $r = 0.005255$ m and $r = 0.01469$ m, respectively. Figures 7 and 8 illustrate the variations of the inelastic strains along the bar at $r = 0.005255$ m and $r = 0.01469$ m, respectively. Figures 9 and 10 show the stresses and the inelastic strains in the radial direction, respectively, at $z = 0.1$ m, where the bar has maximum tensile stresses at the surface. Figures 11 and 12 show the stresses and the inelastic strains in the radial direction, respectively, at $z = 0.6$ m.

In the quenching analysis presented in this paper, the quadrilateral elements with 8 nodes and 4 integration points for the stress problem, and 4 nodes and 4 integration points for the thermal problem are used for both the transient and steady state analysis. For the

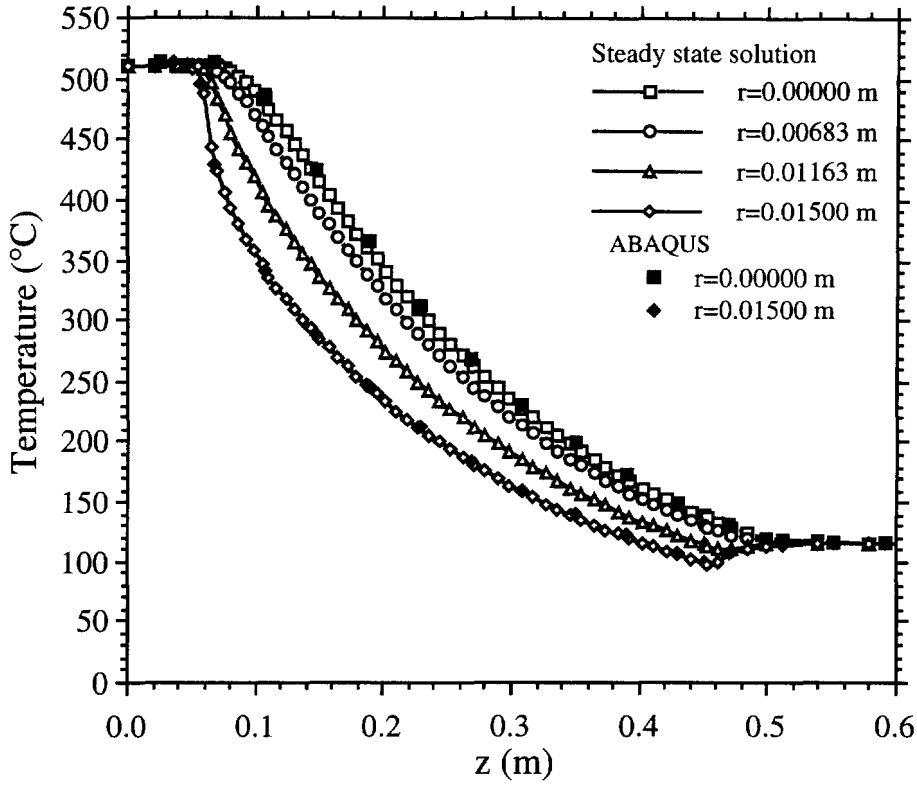

Fig. 2. Temperature distributions along the quenched circular bar at various locations in the radial direction.

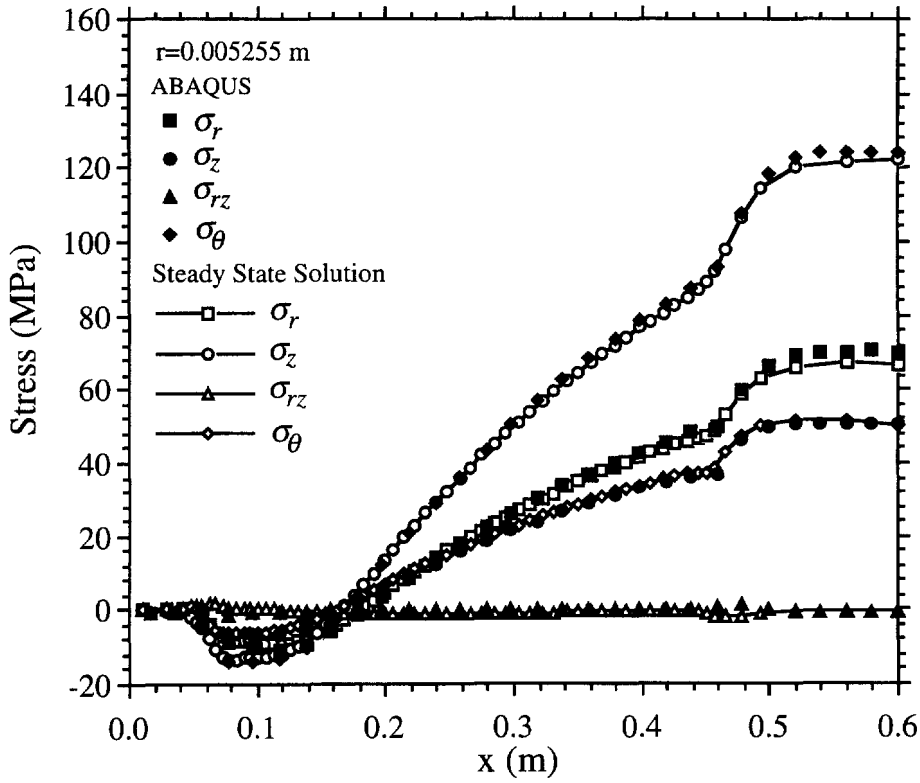

Fig. 3. Stresses along the quenched circular bar near the bar center.

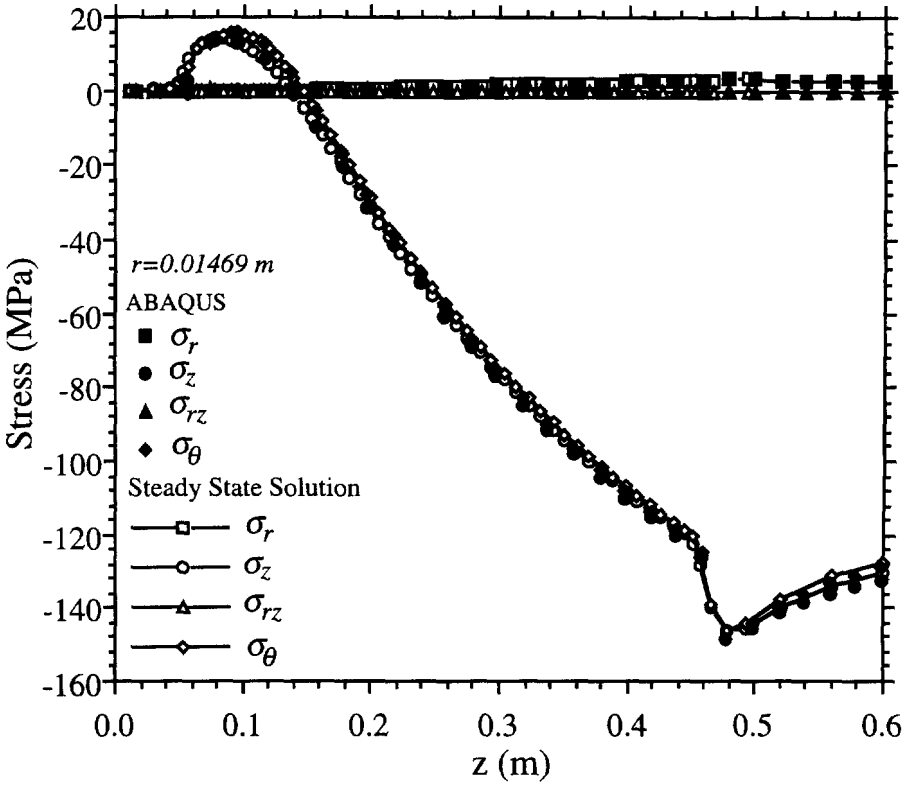

Fig. 4. Stresses along the quenched circular bar near the bar surface.

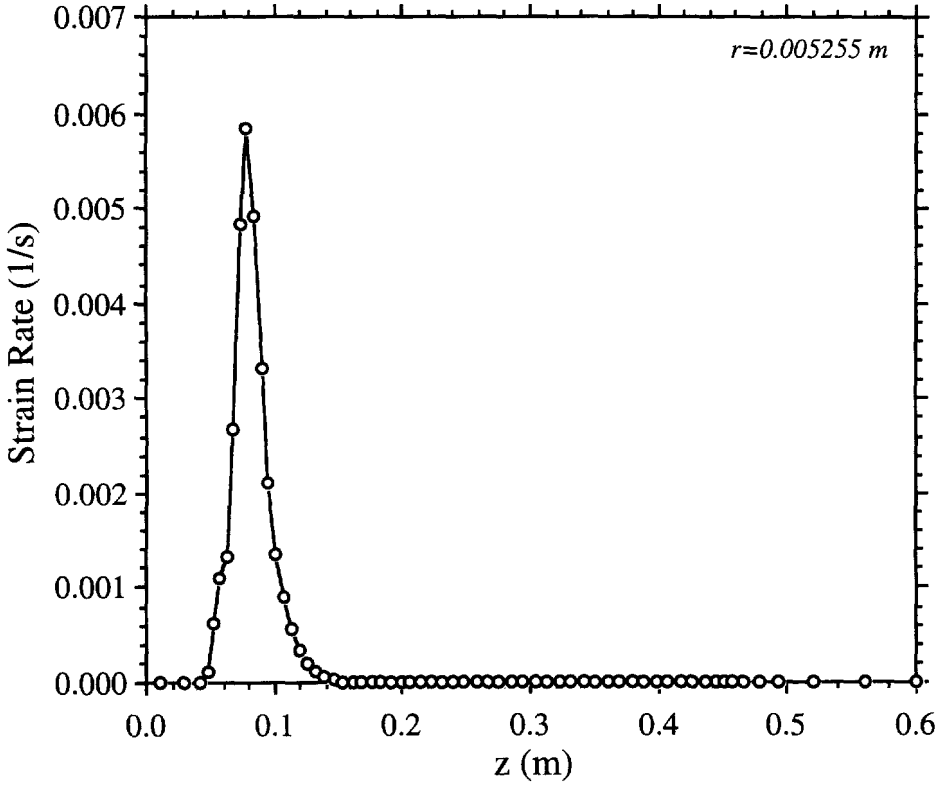

Fig. 5. Inelastic strain rate along the quenched circular bar near the bar center.

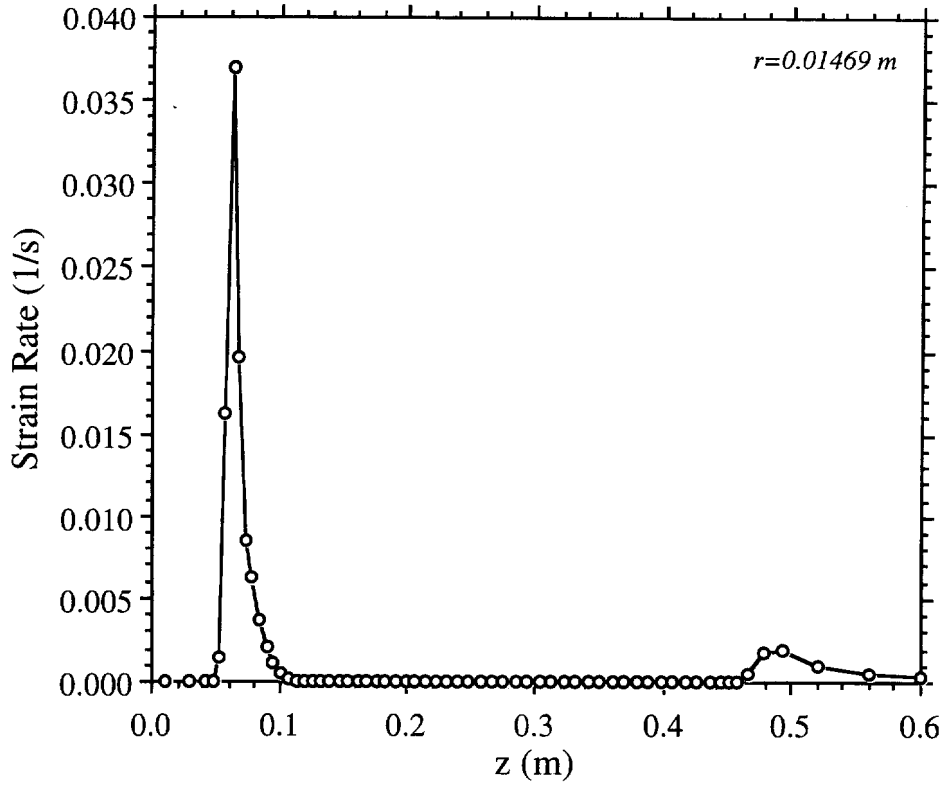

Fig. 6. Inelastic strain rate along the quenched circular bar near the bar surface.

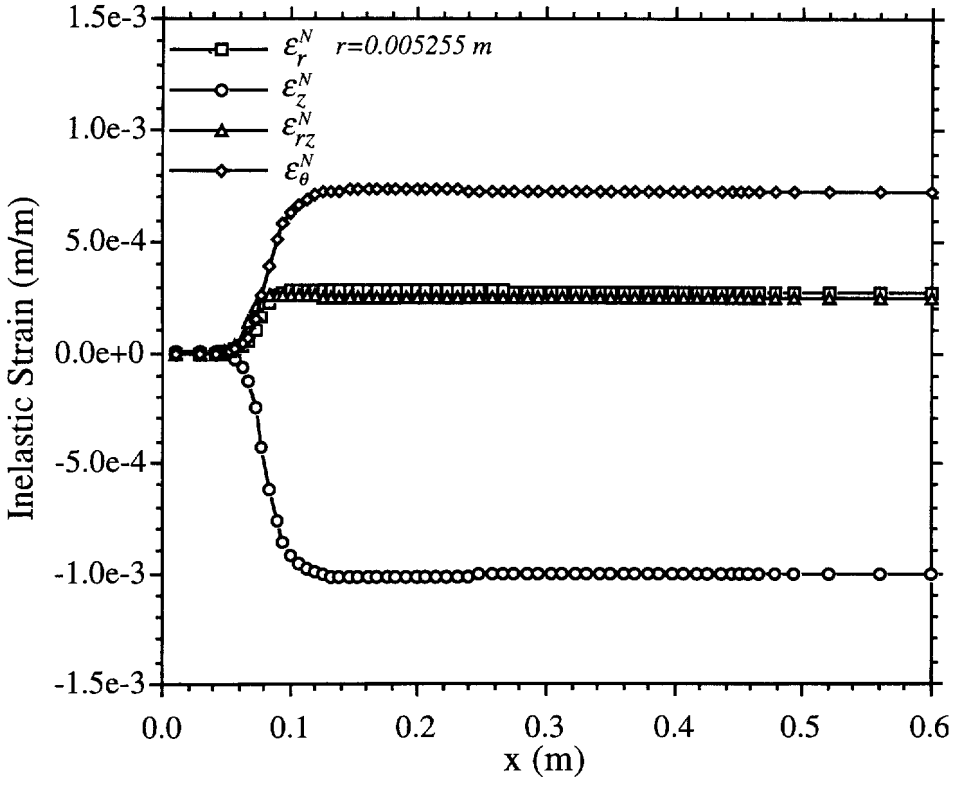

Fig. 7. Inelastic strains along the quenched circular bar near the bar center.

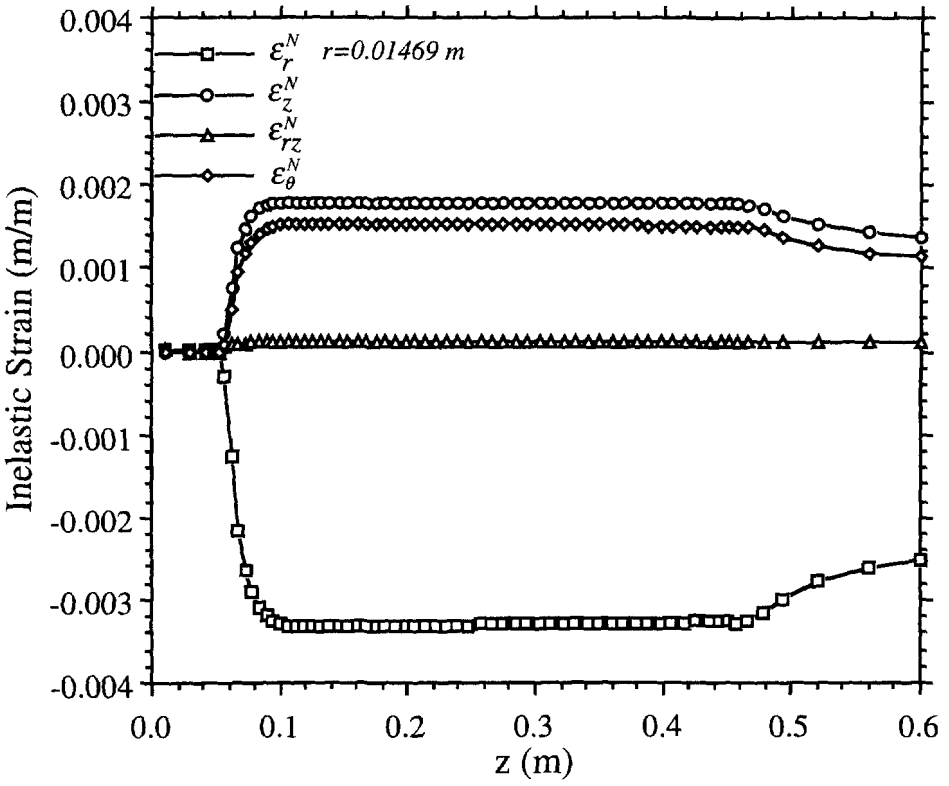

Fig. 8. Inelastic strains along the quenched circular bar near the bar surface.

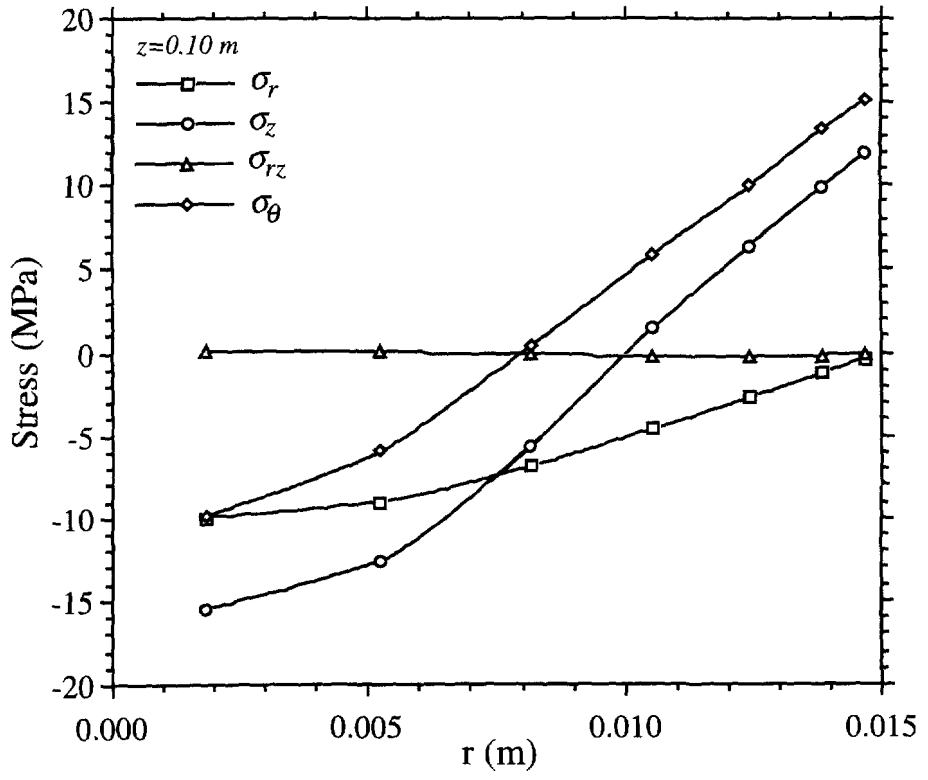

Fig. 9. thermal stresses along the radial direction of the quenched circular bar at $z = 0.1$ m.

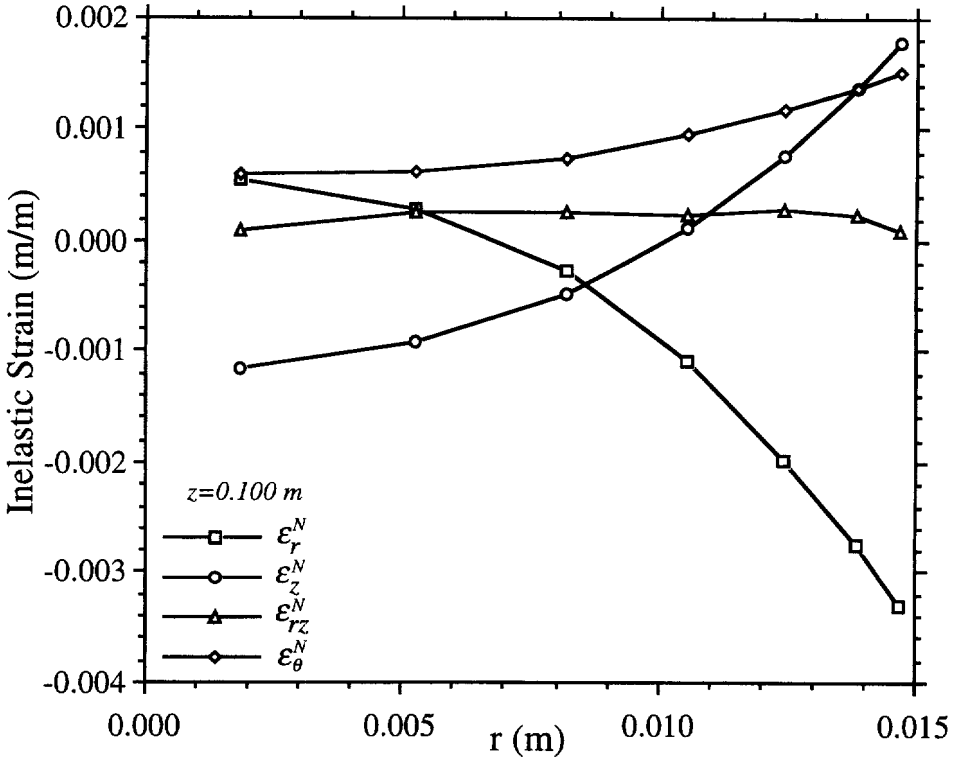

Fig. 10. Inelastic strains in the radial direction of the quenched circular bar at $z = 0.1$ m.

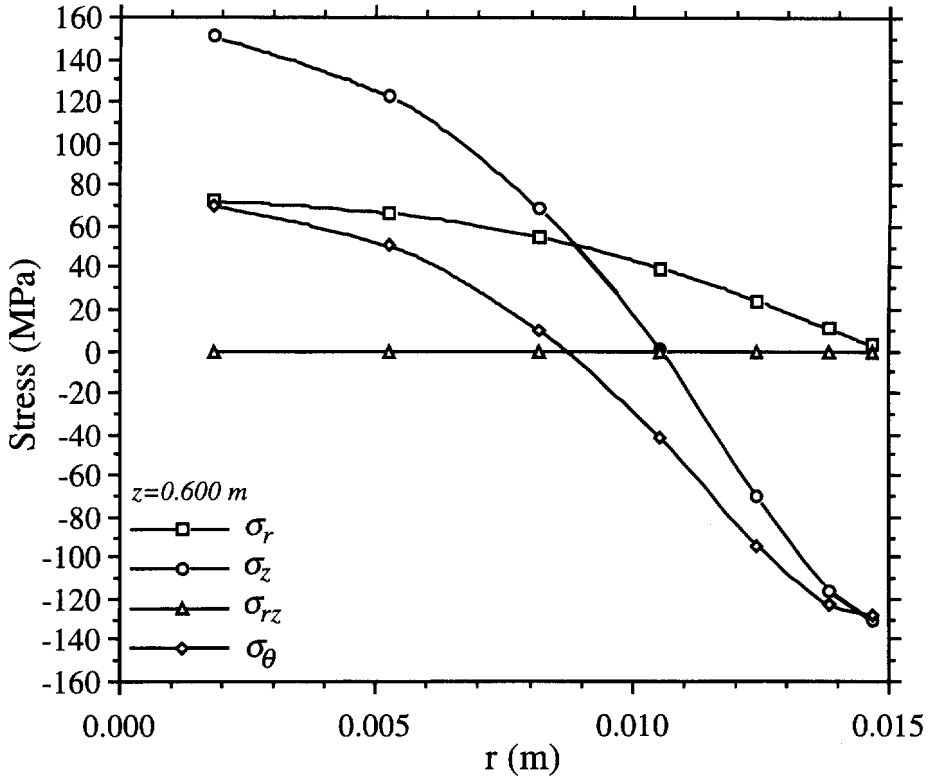

Fig. 11. Thermal stresses along the radial direction of the quenched circular bar at $z = 0.6$ m.

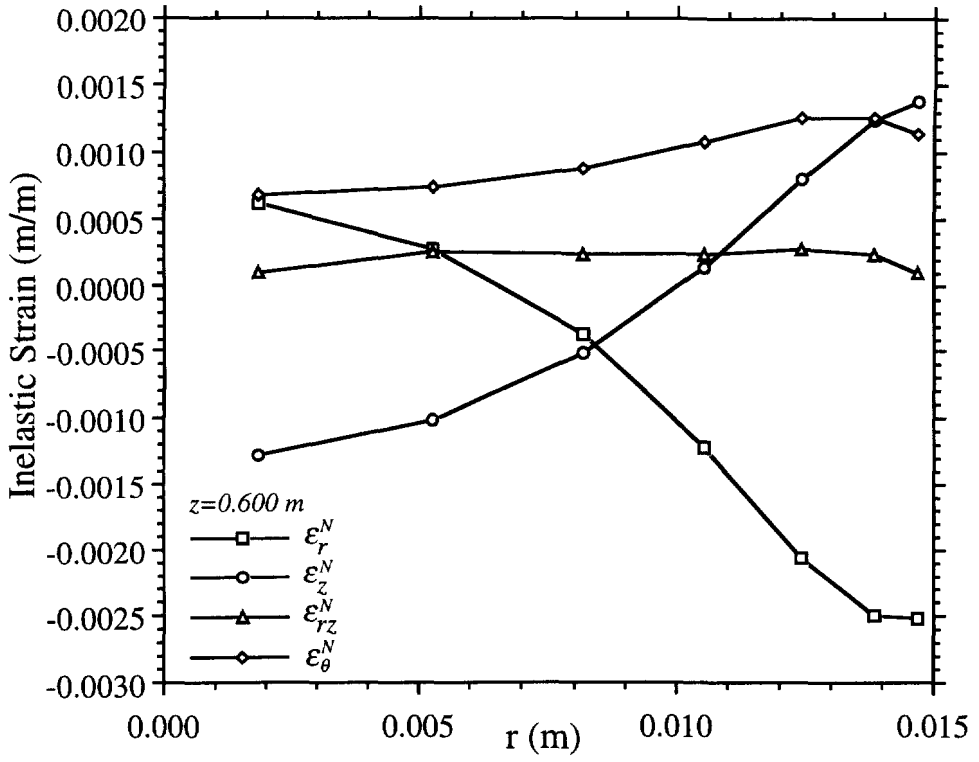

Fig. 12. Inelastic strains in the radial direction of the quenched circular bar at $z = 0.6$ m.

steady state analysis, 455 elements are used with 7 elements in the radial directions. For the analysis with the Lagrangian approach, the cooling zone is fixed and the quenched body is moving. To eliminate the transient and end effects with the Lagrangian method, the length of the bar is selected to be 1 m, where total 995 elements are used with 5 elements in the radia direction. In addition, the elements are carefully generated to minimize the level of computation. For the example problems discussed in this paper, the computational time is about 1.5 CPU hours on hp 750 machine with the present method and about 30 CPU hours with the Lagrangian method (ABAQUS).

CONCLUSION

The general methodology, which is presented in this paper, has been shown to be an effective and efficient tool to analyze the stresses involved in the continuous quenching processes. Large residual stresses in quenched products are highly undesirable. With the present method, one is able to efficiently predict the residual stress pattern and their magnitude in the continuous quenching process. By adjusting the process conditions such as the cooling heat transfer coefficient, the length of the cooling zone, and the traveling speed of the bar, we are able to control and minimize the residual stresses.

According to the Saint Venant principle, the boundary conditions assumed at the upstream and down stream of a control volume will only affect the local stress distribution. Therefore, the control volume should be selected larger than the region where the stresses need to be determined.

Generally, the axial and Hoop stresses in the region close to the bar surface are tensile at the beginning of the quenching process, while these stresses change from tensile to compressive at early stage of the process and stay compressive.

For the alloy studied here, the magnitude of the inelastic strains increases quickly at the beginning of the quenching process, then stay at almost constant level during the rest of cooling process. Several exercises have been done and it is suggested that the residual stresses can be reduced with shorter cooling zone.

To perform the thermal stress analysis for the continuous quenching process with the present method, the computational time needed is an order of magnitude less than that with Lagrangian approaches.

REFERENCES

ABAQUS (1995) Hibbitt, Karlsson & Sorensen, Inc.. Pawtucket, RI.

Becker, R., M. E. Karabin, J. C. Liu, and R. E. Smelser (1994). Experimental validation of predicted distortion and residual stresses in quenched bars. In *ASME Winter Meeting*, Chicago, IL, x–y month.

Fletcher, A. H. and C. Lewis (1985) Effect of free edge on thermal stresses in quenched plates. *Material Science and Technology* **1,** 780–785.

Johnson, C. (1987) *Numerical Solution of Partial Differential Equations by the Finite Element Method.* Cambridge University Press, Cambridge.

Kikuchi, N. (1986) *Finite Element Methods in Mechanics.* Cambridge University Press, Cambridge.

Pironneau, O. (1989) *Finite Element Methods for Fluids.* John Wiley & Sons, Chichester.

Zabaras, N., S. Mukherjee, and W. R. Arthur (1987) A numerical and experimental study of quenching of circular cylinders. *Journal of Thermal Stress* **10,** 177–191.

Zienkiewicz, O. C. and R. L. Taylor (1991) *The Finite Element Method, 4th ed.* McGraw-Hill Book Company, New York.